MATHEMATICS IN ENGINEERING, SCIENCE AND AEROSPACE
MESA - www.journalmesa.com
Vol. 10, No. 4, pp. 681-693, 2019

High-order adaptive control in multi-agent quadrotor formation*

Stanislav Tomashevich [1,2*], Boris Andrievsky[2,3]

[1] ITMO University, 49 Kronverkskiy pr. 197101 Saint Petersburg Russia
[2] Institute of Problems in Mechanical Engineering, the Russian Academy of Sciences
61 V.O. Bolshoy pr. 199178 Saint Petersburg Russia
[3] Saint Petersburg State University, 13B Universitetskaya Emb. 199034 Saint Petersburg Russia

* *Corresponding Author*. E-mail: tomashevich.stanislav@gmail.com

Abstract. In the paper, the high-order adaptive algorithm to controlling the multi-agent system is proposed. Control of the pitch/yaw angles of quadrotors is taken as an example. It is shown that realistic noisy measurement errors of sensors do not affect drastically the overall system performance with the proposed algorithm. The real-word 2DOF laboratory quadrotor testbed was used for demonstrating the trajectories convergence. Consensus achievement in the multi-agent system consisting of four quadrotor testbeds in the noisy sensor case is evaluated by the simulations. It is shown that the proposed technique allows using decentralized cooperative control for the examined multi-agent system. Realistic gyroscope properties were taken into account while studying the noisy measurement case. The series of numerical simulations were performed to validate of proposed multi-agent system performance for the various algorithm parameters.

1 Introduction

Multi-agent systems, consisting of interacting subsystems (agents), are now finding extended application in the various fields [2, 3, 4]. These systems allow to effectively perform tasks that otherwise could not be performed by individual subsystems. The use of decentralized control in multi-agent systems makes it possible to make the system autonomous. Control signals are generated not by a common control center, but by local controllers based on mutual inter-agent information exchange. Given the expansion of the scope of application of miniature autonomous mobile robots, such as light unmanned aerial vehicles (UAVs), autonomous underwater vehicles (AUVs), walking robots, see [5, 6, 7, 8] for mentioning a few, one should consider applicability of more sophisticated control

* The preliminary version has been presented at the 12th International Conference on Mathematical Problems in Engineering, Aerospace and Sciences, ICNPAA 2018, Yerevan, Armenia, 3–6 July 2018, [1].

2010 **Mathematics Subject Classification**: 93C40 93D10 93D21 74F10 37M05
Keywords: multi-agent systems, adaptive control, formation control, quadrotor, noisy sensors

laws for multi-agent systems. The idea of combining agents into groups according to the purposes of the performing tasks, becomes more accessible and effective. An approach and basic principles, used in this rapidly developing field in recent years, allow obtaining systems that work autonomously, taking into account both external and internal factors.

An important property of a multi-agent system is the way to organize interactions between agents. The choice of the network structure through which agents exchange information largely determines the characteristics of the system as a whole. The difficulty in designing multi-agent systems is associated with a large number of agents. One of the main tasks for multi-agent systems is to ensure the convergence of the agents states or outputs to a common value (for example, to the average of the initial states) or a common given trajectory [9, 10].

Development and implementation for practice of multi-agent systems necessitates, first of all, to ensuring the required quality of the system as a whole. Noisy sensors measurements could upset the stability of multi-agent system. Real systems (including UAVs and robots mentioned above) has sensors that are not ideal so there is a plenty of various measurement noises. This should be taken into account while developing multi-agent systems. One of the aim of this work is to demonstrate how stochastic measurement errors affect to multi-agent system with the suggested adaptive control.

The theory of adaptive control began to develop at the end of the last century [11], and today it has a sufficient development, see e.g. [12]. Adaptive control is increasingly being used in areas where not all system parameters can be known. Before one can use it in real systems any control it is necessary to ensure the adequacy of the proposed algorithms by modeling.

The paper uses a modified high order adaptation algorithm that, unlike [13, 14], is configured for stabilization with unknown feedback coefficient. The first adaptation algorithm of high order (high order tuner) was published in [15]. Later it was suggested many modifications of this algorithm, the closest to the one used in the paper are algorithms [16, 17, 18].

With the increasing popularity and availability of the UAV such as quadrotor it becomes possible to implement complex control laws in such miniature, but not simple systems. The most common method is use of stabilizing PID controllers and their modifications, so there is a plenty of works devoted to the design of this type of controllers [19, 20, 21, 22, 23]. The algorithms based on the backstepping method can be found in [24, 25, 26, 27]. Algorithms of other types are discussed in [28, 29, 30, 31, 21, 32, 33].

2 Multi-agent Control

For multi-agent systems, the concept of consensus, which can be considered as one of the types of synchronization, is widely used. One of the earliest examples of consensus behavior is the task of driving cars at the same speed [34, 35, 36]. The coordinate synchronization condition of linear agents can be written as

$$\lim_{t\to\infty} |x_i(t) - x_j(t)| = 0, \quad i, j = 1, \ldots, N, \tag{2.1}$$

where x_i is the state vector of the i-th agent, and N is the number of agents. The condition of generalized coordinate synchronization is set similarly:

$$\lim_{t\to\infty} |y_i(t) - y_j(t)| = 0, \quad i, j = 1, \ldots, N, \tag{2.2}$$

where $y_i(t) = Cx_i(t)$, and C is the output matrix. Note that goals (2.1) and (2.2) imply only synchronizing the state and output vectors of the agents, respectively, and the convergence $x_i(t)$, $y_j(t)$ is not specified for some given process.

Due to the fact that agents must interact with each other, communication between them must be established through the channel of information transfer. For example, this may be information about the position in space of a moving agent. A network structure should also be specified that describes the interaction of agents between themselves. For this purpose, the network topology is usually used in the form of graphs and the corresponding mathematical apparatus is used.

Most often in this area, Laplacian (Laplace matrix) is used, which allows us to move from the visual (in the form of a graph) to a formula description of the interaction. In a more general case, for example, in tracking problems, a connectivity matrix is used to describe the interaction. In the paper, a digraph without loops is considered, in this case all the arcs are directed. The number of arcs entering the vertex α is denoted by $d_i(\alpha)$, and the number of outgoing arcs is denoted by $d_o(\alpha)$. Then the Laplacian is introduced as $L = I - G$, where I is the diagonal identity matrix, and G is the adjacency matrix, formed by the rule

$$\begin{cases} G_{ij} = 1/d_o(\alpha_i), & \text{if } d_o(\alpha_i) \neq 0, \\ G_{ij} = 0, & \text{otherwise}, \end{cases} \tag{2.3}$$

where G_{ij} is the element of the matrix G in the row i and the column j; i, j are the numbers of the corresponding agents. The Laplace matrix obtained in this way characterizes not only the directions and order of interaction, but also the degree of influence of agents on each other. In the simplest form, the dynamics of agents can be described by linear equations. In a paper, a multi-agent system consisting of N linear agents is considered:

$$\dot{x}_i(t) = A_a x_i(t) + B_a u_i(t), \quad y_i(t) = C_a x_i(t), \quad i = 1, \ldots, N, \tag{2.4}$$

where $x_i(t) \in \mathbb{R}^n, u_i(t) \in \mathbb{R}^m, y_i(t) \in \mathbb{R}^l$ are the state, input, and output vectors respectively, for the i-th agent, and A_a, B_a, C_a are matrices of the corresponding sizes. Due to the interaction of agents, a synchronization signal is generated, which is set as follows:

$$z_i(t) = -\Big(y_i(t) - \frac{1}{|J_i|} \sum_{j \in J_i} y_j(t)\Big), \quad i = 1, \ldots, N, \tag{2.5}$$

where $|J_i|$ is the cardinality of the set J_i is the set of incoming arcs. Equation (2.5) sets the consensus protocol, which, together with a certain graph of connections, gives the corresponding Laplacian [2, 37, 38, 39, 40]. The rank of the Laplace matrix of the graph Γ is $N - v$, where v is the forest dimension of the graph over incoming trees. In particular, $\operatorname{rank} L = N - 1$, that is, the zero eigenvalue of the matrix L has unit multiplicity if and only if the digraph Γ has an oriented spanning tree. The latter means that the system does not divide agents into clusters. Information in this case can go to any vertex and there are no separate agents in the system.

For the above problem statement, the following result is known. A multi-agent system consisting of N agents of the form (2.4), controllers in the form of $u_i(t) = z_i(t)$ and consensus protocol (2.5) asymptotically reaches consensus if and only if systems of the following form are simultaneously asymptotically stable

$$\dot{x}_i(t) = A_a x_i(t) + B_a u_i(t), \quad y_i(t) = C_a x_i(t), \quad z_i(t) = \lambda_i y_i(t), \quad i = 1, \ldots, N, \tag{2.6}$$

where λ_i, $i = 1, 2, \ldots, N$ are the eigenvalues of the Laplacian L for a given graph of connections [41].

Adaptive control could be used for solving consensus problem [42]. For each agent the dynamic is described as

$$Q_i(p) y_i(t) = k_i R_i(p) u_i(t), \quad i \in \overline{1, N}, \tag{2.7}$$

where $y_i(t)$ and $u_i(t)$ are the scalar output and input signals of the i-th agent, respectively, $p = d/dt$ is the differentiation operator, $R_i(p)$ and $Q_i(p)$ are linear differential operators with unknown coefficients belonging to the well-known bounded set Ξ, $\deg R_i(p) = m$ and $\deg Q_i(p) = n$, $R_i(\cdot)$ are Hurwitz polynomials, $n - m \geqslant 1$, $k_i > 0$ are coefficients whose values are in the set Ξ.

For each agent, a leading subsystem is defined that determines its reference movement trajectory:

$$Q_m(p)y_{mi}(t) = k_m R_m(p)z_i(t), \quad i \in \overline{1,N}, \tag{2.8}$$

where $y_{mi}(t)$ is the output of the leading subsystem, $z_i(t)$ is the reference signal generated for each agent and depending on the state of other agents. Using this approach allows to assign each of the agents (the dynamics of which may be different) the same reference leading subsystem. Setting the consensus protocol (2.5) to form the input $z_i(t)$ of the reference model (2.8) allows us to obtain a model of a closed multi-agent system in a classical form.

The control aim is expressed by the following objective condition

$$\overline{\lim_{t\to\infty}}|y_i(t) - y_{mi}(t)| < \delta, \quad i \in \overline{1,N} \tag{2.9}$$

and consensus for outputs

$$\overline{\lim_{t\to\infty}}|y_i(t) - y_j(t)| < 2\delta, \quad i,j \in \overline{1,N}, \tag{2.10}$$

as well as the limitations of all signals in a closed-loop system. Here $\delta > 0$ is the control accuracy in the steady state. In the synthesis of the control law, the eigenvalues of the Laplacian are not used. It is important to note the features of the task: it is believed that the communication channel through which information is transmitted is ideal. This means that one can neglect the limitations of its bandwidth, time quantization, disappearance and delay of data packets and other distortions inherent in real communication channels.

3 Setup Description

As it was mentioned above, multi-agent control can be used for UAVs for the different purposes. In the following sections for the sake of clarity we focus our attention to real-world quadrotor test-bed. The future researches are planned to do with a real multi-agent system based on the set of these test-beds.

For in-flight tests the spacious area, which is free from different obstacles is needed. Also, the flight testing procedure is rather time consuming for the researchers. To overcome the mentioned problems at the initial stage of real-world adaptive controllers design the laboratory testbed has been used. The testbed allows to safely test new control algorithms in the small space laboratory area and promptly make changes in the cases of failure.

The main part of the test-bed is the miniature quadrotor, which is installed on the 2DOF gimbal suspension, allowing the helicopter to freely rotate on pitch and roll. The outer frame is mounted on the pillars and can rotate about the horizontal axis. The inner gimbal frame can rotate with respect to the outer one. Helicopter is fixed in the middle of the inner frame. The helicopters center of mass is fixed, eliminating an opportunity of unforeseen changes and the dangerous trajectory. Pillars are mounted on the square support. The whole construction is made from wood and metal angle braces. In details test-bed is presented in [43].

The tested 2DOF quadrotor is based on radiating frame DJI 450 and supplied with Ardupilot Mega 2.6 autopilot with the IMU, the GPS the satellite navigation system, see [44] for more details. The brush-less motors with external rotor DJI 2213 (250 W each) are used as actuators. The device is

supplied with the Electronic Speed Controllers (ESC) DJI 30A Opto with current output up to 30 A and with operating voltages up to 14.8 V, rotors left and right rotation with the size 10×4.5 or 8×4.5 inches. The real-time data exchange with the operator's PC is fulfilled by means of the WiFi XBee modem.

Quadrotor dynamics can be described as follows:

$$\begin{cases} m\dot{V}_x = \tau_y(C_\psi S_\vartheta C_\gamma + S_\psi S_\gamma) - V_x A_x, \\ m\dot{V}_y = -mg + \tau_y(C_\vartheta C_\gamma) - V_y A_y, \\ m\dot{V}_z = \tau_y(S_\psi S_\vartheta C_\gamma - C_\psi S_\gamma) - V_z A_z, \\ \dot{\gamma} = \omega_x + S_\gamma T_\vartheta \omega_z + C_\gamma T_\vartheta \omega_y, \\ \dot{\vartheta} = C_\gamma \omega_z - S_\gamma \omega_y, \\ \dot{\psi} = \dfrac{S_\gamma}{C_\vartheta}\omega_z + \dfrac{C_\gamma}{C_\vartheta}\omega_y, \\ I_x\dot{\omega}_x = (I_y - I_z)\omega_y\omega_z - I_r\omega_z\omega_r + \tau_\gamma, \\ I_y\dot{\omega}_y = (I_z - I_x)\omega_x\omega_z + \tau_\psi, \\ I_z\dot{\omega}_z = (I_x - I_y)\omega_x\omega_y + I_r\omega_x\omega_r + \tau_\vartheta, \end{cases} \tag{3.1}$$

where V_x, V_y, V_z are linear velocities along the respective axes, τ_y, τ_γ, τ_ϑ, τ_ψ are the control inputs, I_x, I_y, I_z denote rotational moments of inertia along X, Y and Z axes respectively, $\omega_x, \omega_y, \omega_z$ stand for the angular velocities around axes X, Y and Z respectively, A_x, A_y, A_z are the aerodynamic coefficients for corresponding axes, ω_r is the average rotational speed of the screws, I_r is the rotor moment of inertia, g denotes the gravity acceleration, γ is the roll angle, ψ is the pitch angle and ϑ stands for yaw angle, $S_\alpha = \sin(\alpha)$, $C_\alpha = \cos(\alpha)$, $T_\alpha = \tan(\alpha)$. Schematics of the quadrotor is shown in Fig. 1.

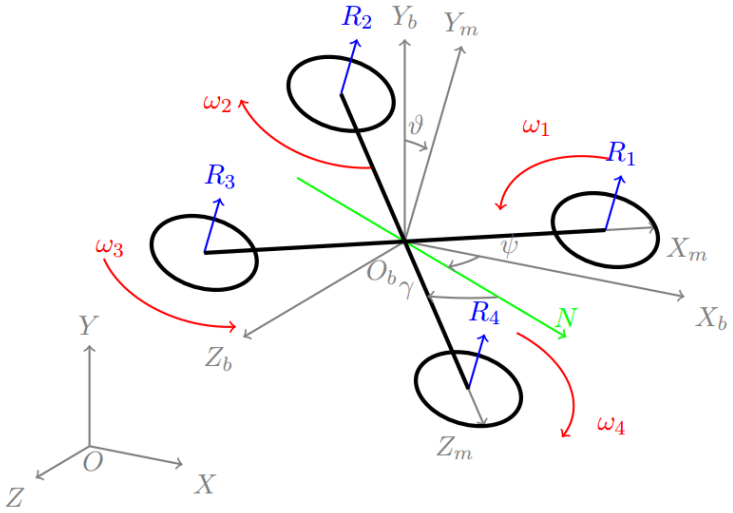

Fig. 1 Schematics of the quadrotor

4 High-order Control Law

Based on the procedure described in [42], the following steps were made to derive the multi-agent version of the original adaptive control law. Without loss of generality, let us assume that adaptive control is applied solely to roll angle (the similar considerations may be done for pitch angle control loop) and use the following single-agent model:

$$\dot{\gamma} = \omega_x + S_\gamma T_\vartheta \omega_z + C_\gamma T_\vartheta \omega_y; \quad I_x \dot{\omega}_x = (I_y - I_z)\omega_y \omega_z - I_r \omega_z \omega_r + \tau_\gamma. \tag{4.1}$$

It is obvious that $\dot{\gamma} = \omega_x$ due to the fact that the motion is considered only with changing angle γ and zero values of the other angles. Then the equation of motion can be written as follows:

$$\ddot{\gamma} = -\beta\dot{\gamma} + \tau_\gamma / I_x, \tag{4.2}$$

where β is the viscous friction gain with respect to the rotation of the testbed about the outer frame.

Represent equation (4.2) in the following form:

$$Q(p)y(t) = kR(p)u(t), \tag{4.3}$$

where $y(t) = \gamma$ and $u(t) = \tau_\gamma$ are the scalar input and output signals respectively, $R(p) = 1$ and $Q(p) = p^2 + \beta p$ are linear differential operators with unknown coefficients, $k = 1/I_x > 0$ is an unknown factor, $p = d/dt$ denotes the differential operator on time. The coefficients of operator polynomials $R(p)$, $Q(p)$ and gain $k > 0$ belong to a known manifold Ξ. Define the *leading subsystem* model as follows

$$Q_m(p)y_m(t) = k_m R_m(p)z(t), \tag{4.4}$$

where $y_m(t)$ is the leading subsystem output, $z(t)$ denotes the reference signal, $Q_m(p) = p^2 + k_1 p + k_2$, $R_m(p) = 1$, $k_m = k_2$. The goal is to derive continuous control law, ensuring fulfillment of (2.9) and (2.10). In the other words, stabilization of $y(t)$ as well as limitations in the steady state mode of all signals in a closed-loop system, where $\delta > 0$ is the prescribed control accuracy, are required.

Let us define $z(t) = -\lambda y(t)$, where λ is an unknown feedback gain. This situation is possible when the feedback controller is already synthesized and it is unknown.

According to [13], define a following control law

$$u(t) = T(p)\hat{v}(t), \tag{4.5}$$

where $T(p)$ is selected so that the transfer function $R_m(s)T(s)/Q_m(s)$ satisfies the strict positive realness condition, $\hat{v}(t)$ denotes the estimate of the auxiliary control $v(t)$:

$$v(t) = c^{\mathrm{T}}\omega(t), \tag{4.6}$$

where $c(t)$ is the vector of adjustable parameters:

$$\dot{c}(t) = -\alpha e(t)\omega(t), \tag{4.7}$$

with a certain $\alpha > 0$. Control law (4.5) ensures the target conditions (2.9), $e(t) = y(t) - y_m(t)$, $\omega(t) = \left[V_1^{\mathrm{T}}(t)\ y(t)\ V_2^{\mathrm{T}}(t)\ (k_m/T(p))y_i(t)\right]^{\mathrm{T}}$ is the regressor. The following filters that are used:

$$\dot{V}_1(t) = F_1 V_1(t) + b\hat{v}(t); \quad \dot{V}_2(t) = F_2 V_2(t) + by(t), \tag{4.8}$$

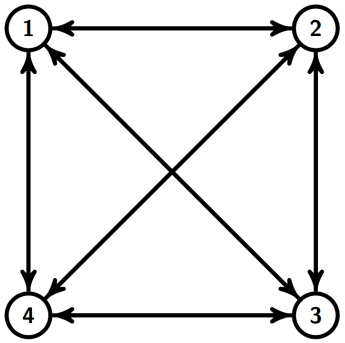

Fig. 2 Complete connectivity graph associated with Laplacian L

where matrices F_1, F_2 are of Frobenius form with the characteristic polynomials $R_m(p)$ and $R_m(p)T(p)$ respectively, $b = \begin{bmatrix}0 \ldots 0\ 1\end{bmatrix}^{\mathrm{T}}$.

To implement control law (4.5) the observer of [45] is employed, which is specified in the form of

$$\dot{\zeta}(t) = G_0\zeta(t) + B(\hat{v}(t) - v(t)); \quad \hat{v}(t) = \mathcal{L}\zeta(t), \tag{4.9}$$

where $\zeta(t) \in \mathbb{R}^{\gamma}$,

$$G_0 = \begin{bmatrix}0 & I_{\gamma-1}\\ 0 & 0\end{bmatrix}, B = \begin{bmatrix}-\dfrac{d_1}{\mu} \ldots -\dfrac{d_\gamma}{\mu^\gamma}\end{bmatrix}^{\mathrm{T}}, \mathcal{L} = \begin{bmatrix}1\ 0 \ldots 0\end{bmatrix}$$

and $d_1, \ldots, d_\gamma$ are selected so that the matrix $G = G_0 + \begin{bmatrix}d_1 \ldots d_\gamma\end{bmatrix}^{\mathrm{T}}\mathcal{L}$ is Hurwitz, $\mu > 0$ is a sufficiently small number. The attainability proof is given in [13]. The special case is considered in [42].

5 Simulation Results

Let us form the control system for polynomials, corresponding to model (4.2) and the parameters, obtained by the identification procedure of [46]: $\beta = 0.397$, $1/I_x = 0.016$. Initial states for quadrotors were set to:

$$x_1(0) = \begin{bmatrix}10\\ -0.3\end{bmatrix}; \quad x_2(0) = \begin{bmatrix}-5\\ -0.4\end{bmatrix}; \quad x_3(0) = \begin{bmatrix}-10\\ 0.6\end{bmatrix}; \quad x_4(0) = \begin{bmatrix}0\\ 0.8\end{bmatrix}. \tag{5.1}$$

The reference model is defined by transfer function

$$W_e(s) = \frac{4.71^2}{s^2 + 9.42s + (4.71)^2}, \tag{5.2}$$

that provides settling time about 1 second after the adaptation process is finished. Based on the properties of reference model (5.2), $T(p)$ can be chosen in the form $T(p) = p + 1$.

The built-in IMU for *Ardupilot Mega 2.6* controller *MPU-6000* is taken in a view for implementation. As it noticed in the specification [47] gyroscope, its noise performance is characterized by root-mean-squared value of the fluctuations $\sigma_{\mathrm{GY}} = 0.05\mathrm{deg}/s$. The highest frequency that developer could use with this autopilot is 100 Hz, so let us use this parameter as the noise generator sampling frequency. Let us consider that result angle could be obtained with numerical integration by trapezoidal rule:

$$\hat{y}_i[k+1] = \hat{y}_i[k] + (\overline{\omega}_i[k+1] + \overline{\omega}_i[k])T/2, \quad i \in \overline{1,N}, \tag{5.3}$$

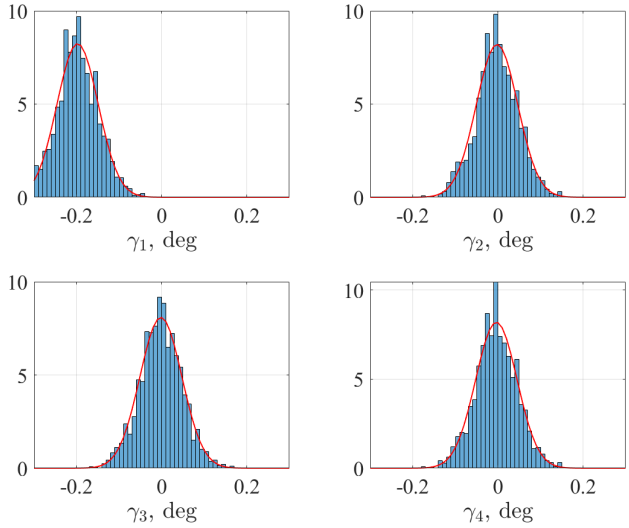

Fig. 3 Probability distribution of agents position in steady state for the case α_1

where $\overline{\omega}_i[k]$ denotes the gyro measurements of the angular velocity at step k with the time period $T = 0.01$ s for each i-th agent. Due to the presence of the measurement errors, the measured angular velocity has additional noise:

$$\overline{\omega}_i[k] = \omega_i[k] + \eta_i, \quad i \in \overline{1,N}, \tag{5.4}$$

where η_i have normal distribution with zero mean value and variance $D_{GY} = (0.05)^2$ (deg/s)^2. Here we could define estimation errors as $e_i[k] = \hat{y}_i[k] - y_i[k]$. The following adaptation gains were chosen for different simulations runs: $\alpha_1 = -0.0001$ and $\alpha_2 = -0.00025$.

The complete graph was chosen as the formation connectivity graph, see Fig. 2, which corresponds to the following connectivity matrix

$$L = \begin{bmatrix} 1 & -1/3 & -1/3 & -1/3 \\ -1/3 & 1 & -1/3 & -1/3 \\ -1/3 & -1/3 & 1 & -1/3 \\ -1/3 & -1/3 & -1/3 & 1 \end{bmatrix}. \tag{5.5}$$

Figs. 3 and 4 show the simulation results for α_1 and α_2 respectively. At time duration $t = 30$ s absolute position of the each agent was stored. Simulation was repeated 10000 times for both α_i and resulting histograms show that measurement noise does not sufficiently affect to reaching conditions (2.9) and (2.10). As it shown at Fig. 5, at the time moment $t = 30$ s all transients are closed to be stabilized even with small control coefficient α_1.

Fig. 7 presents estimation errors. Here one could see noisy angle measurements caused by noisy gyroscope. This measurements was obtained just by using numerical integration of noisy angular velocity measurements. In common case this integral should infinitely increase, but due to the fact that every agent has feedback through other agents, the angles estimations are close to the real signals.

As one can see from Fig. 6 adaptation process has finished about $t = 20$ s and after this time moment agents start moving with dynamic given with model (5.2). The same result (but more faster) could be obtained with more robust case with α_2.

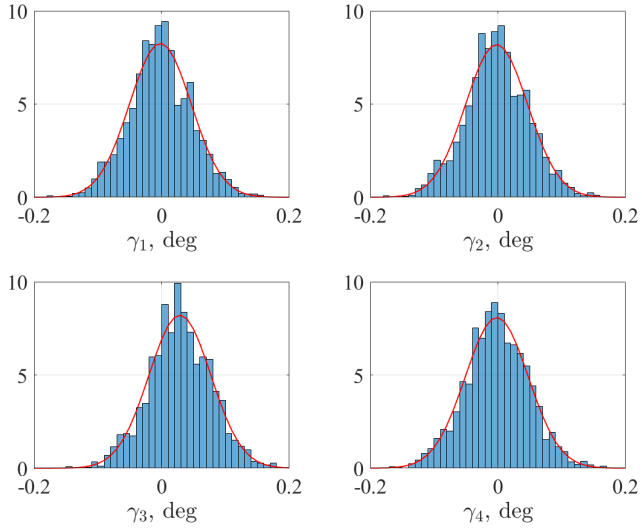

Fig. 4 Probability distribution of agents position in steady state for the case α_2

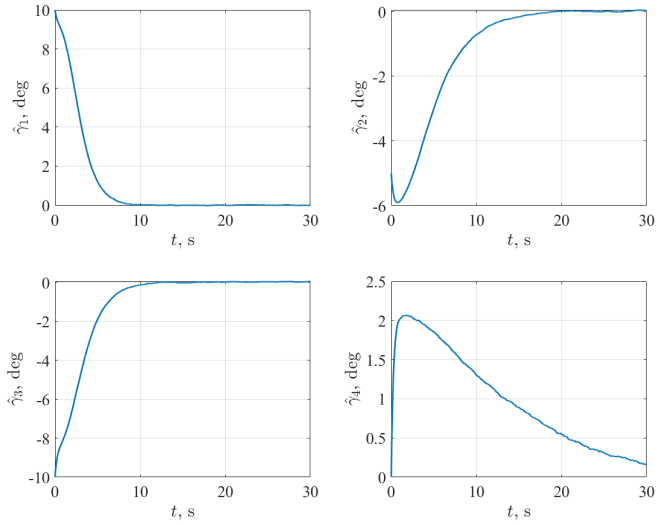

Fig. 5 Agents trajectories for the case α_1

Proposed adaptive control for quadrotor shows good results within acceptable angles. It can be seen that result does not depend on λ_i and its sign. Moreover only one parameter α can change the quality of transients. In Tab. 1 output signals statistical properties are presented. Non-zero mean value for the first agent with α_1 means that control algorithm is not robust enough. In case of α_2 trajectories tends to each other more closer. Moreover, one could see that standard deviations match with settled sensors noise deviations. This leads us to conclusion that the proposed algorithms satisfy conditions (2.9) and (2.10) even with noisy sensors measurements.

Table 1 Statistical properties of system outputs

	Mean value		Standard deviation	
Agent number	α_1	α_2	α_1	α_2
# 1	−0.1975	−0.0021	0.0484	0.0483
# 2	−0.0020	−0.0020	0.0486	0.0487
# 3	−0.0018	0.0286	0.0493	0.0486
# 4	−0.0036	−0.0018	0.0487	0.0493

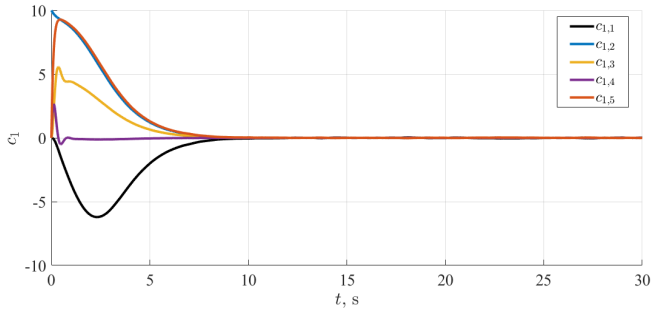

Fig. 6 Transients of the vector c_1 components for the case α_1

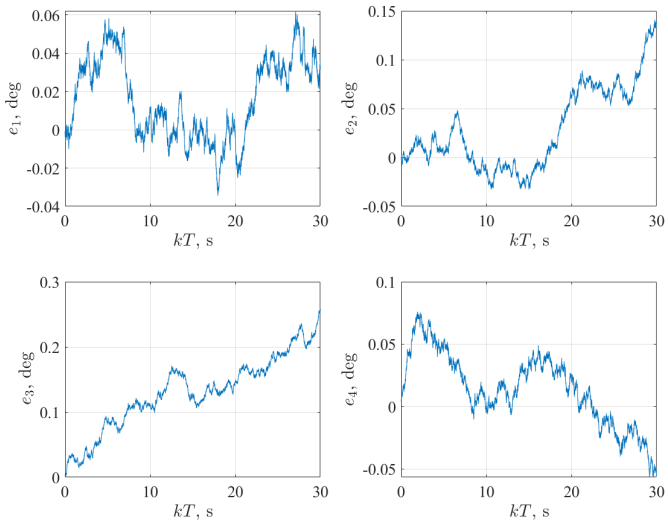

Fig. 7 Estimation error for the case α_1

6 Conclusion

In this paper the possibility to use a high order adaptation algorithm to control multi-agent system with noisy sensors is presented. As an example it was show for the case of synchronizations quadrotors angles on laboratory testbeds. System parameters used in this paper was previously received with identification algorithms. Noise parameters are based on real IMU system used in quadrotors. A numerical simulation is given and it is showing adequacy of the results with using this algorithm with real system.

Acknowledgments

Designing the formation adaptive control law was supported by RFBR, grant 18-38-20037. Computer simulations of the adaptive system were supported by RFBR, grant 17-08-01728.

References

[1] S. Tomashevich and B. Andrievsky. Adaptive control of quadrotors spatial motion in formation with implicit reference model. *AIP Conference Proceedings*, 2046:020103–(1-10), 2018.

[2] A. V. Proskurnikov and A. L. Fradkov. Problems and methods of network control. *Automation and Remote Control*, 77(10):1711–1740, 2016.

[3] F. L. Lewis, H. Zhang, K. Hengster-Movric, and A. Das. *Cooperative control of multi-agent systems: optimal and adaptive design approaches*. Springer, 2014.

[4] Z. Li and Z. Duan. *Cooperative control of multi-agent systems: A consensus region approach.* CRC Press, 2014.

[5] M. Porfiri, D. G. Roberson, and D. J. Stilwell. Tracking and formation control of multiple autonomous agents: A two-level consensus approach. *Automatica*, 43(8):1318–1328, 2007.

[6] W. Ni and D. Cheng. Leader-following consensus of multi-agent systems under fixed and switching topologies. *Systems & Control Letters*, 59(3–4):209–217, 2010.

[7] Z. Li, W. Ren, X. Liu, and M. Fu. Distributed containment control of multi-agent systems with general linear dynamics in the presence of multiple leaders. *Int. J. Robust and Nonlinear Control*, 23:534–547, 2013.

[8] H. Ahmed, R. Ushirobira, D. Efimov, L. Fridman, and Y. Wang. Oscillatory global output synchronization of nonidentical nonlinear systems. *IFAC-PapersOnLine*, 50(1):2708–2713, 2017.

[9] R. Olfati-Saber. Flocking for multi-agent dynamic systems: Algorithms and theory. *IEEE Trans. Automat. Contr.*, 51(3):401–420, 2006.

[10] R. O. Saber and R. Murray. Flocking with obstacle avoidance: cooperation with limited communication in mobile networks. In *Proc. 42nd IEEE Conf. Decision and Control (CDC 2003)*, volume 2, pages 2022–2028, 2003.

[11] K. J. Astrom and B. Wittenmark. *Adaptive control*. Addison-Wesley Longman Publishing Co., 1994.

[12] I. Barkana. *Adaptive control? But is so simple!* Journal of Intelligent & Robotic Systems. 83(1):3–34, 2016.

[13] I. B. Furtat and A. M. Tsykunov. Adaptive control of plants of unknown relative degree. *Automation and Remote Control*, 71(6):1076–1084, 2010.

[14] I. B. Furtat and A. M. Tsykunov. An adaptive control output synthesis for the systems with delay on the basis of modified high order algorithm. *Pribor. Sist., Upravlen. Kontr. Diagn.*, pages 15–17, 2006.

[15] A. S. Morse. High-order parameter tuners for the adaptive control of nonlinear systems. *Isidori A., Tarn T. J. (eds.) Systems, Models and Feedback: Theory and Applications*, pages 339–364, 1992.

[16] A. M. Tsykunov. A modified high-order adaptive output feedback control algorithm for linear plants. *Automation and Remote Control*, 67(8):1311–1321, 2006.

[17] A. L. Fradkov, I. V. Miroshnik, and V. O. Nikiforov. *Nonlinear and adaptive control of complex systems*. Springer, 1999.

[18] V. O. Nikiforov and A. L. Fradkov. Adaptive control schemes with extended error. *Automation and Remote Control*, 55(9):1239–1255, 1994.
[19] H. Bolandi, M. Rezaei, R. Mohsenipour, H. Nemati, and S. M. Smailzadeh. Attitude control of a quadrotor with optimized PID controller. *Intelligent Control and Automation*, 4:335–342, 2013.
[20] J.C.V. Junior, J.C. De Paula, G.V. Leandro, and M.C. Bonfim. Stability control of a quad-rotor using a PID controller. *Brazilian Journal of Instrumentation and Control*, (1):15–20, 2012.
[21] T. Luukkonen. Modelling and control of quadcopter. resreport, Aalto University, 2011.
[22] M. Z. Mustapa. Altitude controller design for quadcopter UAV. *Jurnal Teknologi (Sciences & Engineering)*, 74(1):181–188, 2015.
[23] G. Szafranski and R. Czyba. Different approaches of PID control UAV type quadrotor. In *Proc. International Micro Air Vehicles Conference, 2011 summer edition*, pages 70–75, 2011.
[24] S. Bouabdallah and R. Siegwart. Backstepping and sliding-mode techniques applied to an indoor micro quadrotor. In *Proc. IEEE International Conference on Robotics and Automation* , Barcelona, pages 2247–2252, 2005.
[25] T. Madani and A. Benallegue. Backstepping control for a quadrotor helicopter. In *Proc. IEEE/RSJ International Conference on Intelligent Robots and Systems*, Beijing, 2006.
[26] T. Madani and A. Benallegue. Control of a quadrotor mini-helicopter via full state backstepping technique. In *Proc. IEEE Conference on Decision and Control*, San Diego, pages 1515–1520, 2006.
[27] H. Zhen, X. Qi, and H. Dong. An adaptive block backstepping controller for attitude stabilization of a quadrotor helicopter. *Wseas Transactions on Systems and Control*, 8(2):46–55, 2013.
[28] B. J. Emran and A. Yesildirek. Robust nonlinear composite adaptive control of quadrotor. *International Journal of Digital Information and Wireless Communications*,4(2):213-225, 2014.
[29] Z. Fang, W. Gao, and L. Zhang. Robust adaptive integral backstepping control of a 3-DOF helicopter. *International Journal of Advanced Robotic Systems*, 9(79):1–8, 2012.
[30] J. Gvoth, M. Blaho, and T. Mudrakova. Parameters optimization for unmanned aerial vehicle control. In *Proc. 22nd Annual Conference In Technical Computing*, Bratislava, pages 27–36, 2014.
[31] T. Lee, M. Leok, and N. H. McClamroch. Geometric tracking control of a quadrotor UAV on SE(3). *Proc. 49th IEEE Conference on Decision and Control*, pages 5420–5425, 2010.
[32] C. Nicol, C. J. B. Macnab, and A. Ramirez-Serrano. Robust neural network control of a quadrotor helicopter. *Proc. Canadian Conference on Electrical and Computer Engineering*, pages 1233–1238, 2008.
[33] D. Peaucelle, A. L. Fradkov, B. Andrievsky, and V. Mahout. Robust simple adaptive control with relaxed passivity and PID control of a helicopter benchmark. *Proc. 18th IFAC World Congress*, Milano, pages 2315–2320, 2011.
[34] D. C. Gazis, R. Herman, and R. W. Rothery. Nonlinear follow-the-leader models of traffic flow operations research. *Operation Research*, (9):545–567, 1961.
[35] R. E. Chandler, R. Herman, and E. W. Montroll. Traffic dynamics: studies in car following. *Oper. Res. Informs.*, (6):165–184, 1958.
[36] G. F. Newell. Nonlinear effects in the dynamics of car following. *Operations Research*, 9(2):209–229, 1961.
[37] R. Olfati-Saber and R. Murray. Consensus problems in networks of agents with switching topology and time-delays. *IEEE Trans. Automat. Contr.*, 49(9.):1520–1533, 2004.

[38] W. Ren and R. W. Beard. *Distributed consensus in multi-vehicle cooperative control*. Springer, 2008.

[39] R. Olfati-Saber, J. A. Fax, and R. M. Murray. Consensus and cooperation in network multi-agent system. *Proc. IEEE*, 95:215–233, 2007.

[40] P. Yu. Chebotarev and R. P. Agaev. Coordination in multiagent systems and Laplacian spectra of digraphs. *Automation and Remote Control*, 70(3):469–483, Mar 2009.

[41] J. A. Fax and R. M. Murray. Information flow and cooperative control of vehicle formations. *IEEE Trans. Automat. Contr.*, 8:1465–1476, 2004.

[42] S. I. Tomashevich. Control for a system of linear agents based on a high order adaptation algorithm. *Automation and Remote Control*, 78(2):276–288, Feb 2017.

[43] A. O. Belyavskyi, S. I. Tomashevich, and B. R. Andrievsky. Application of 2DOF quadrotor-based laboratory testbed for engineering education. *Proc. 25th Mediterranean Conference on Control and Automation*, pages 939–944, 2017.

[44] S. Tomashevich and B. Andrievsky. Stability and performance of networked control of quadrocopters formation flight. *Proc. 6th Int. Congress on Ultra Modern Telecommunications and Control Systems*, St. Petersburg, pages 331–336, 2014.

[45] A. N. Atassi and H. K. Khalil. A separation principle for the stabilization of class of nonlinear systems. *IEEE Trans. on Automat. Control*, 44(9):1672–1687, 1999.

[46] S. I. Tomashevich, A. O. Belyavskyi, and B. Andrievsky. Control and identification experiments on 2DOF laboratory helicopter setup. In *Proc. 12th IFAC International Workshop on Adaptation and Learning in Control and Signal Processing*, Eindhoven, 2016.

[47] MPU-6000 and MPU-6050 Product Specification., August 2013. Rev. 3.4.